# Experimental Study of Particle Production at Small Angles in Nucleon-Nucleon Collisions at 19 and 23 GeV/$c$†

D. DEKKERS, J. A. GEIBEL, R. MERMOD, G. WEBER,* T. R. WILLITTS, AND K. WINTER
*CERN, Geneva, Switzerland*

B. JORDAN AND M. VIVARGENT
*Institut du Radium, Orsay, France*

AND

N. M. KING AND E. J. N. WILSON
*Rutherford High Energy Laboratory, Chilton, England*

(Received 13 July 1964)

Differential cross sections are presented for the production of pions, kaons, protons, and antiprotons at the angles 0° and 5.7°, produced in proton collisions with $H_2$, Be, and Pb targets at primary momenta of 18.8 and 23.1 GeV/$c$, and in some cases at 8.65 and 11.8 GeV/$c$. The data are discussed with special reference to the role of isobar excitation in the production of secondary particles. All qualitative features of the experimental data are shown to be consistent with a dominant role of isobar decay in the production of pions, positive kaons, and protons at small angles. Excitation of isobars is shown to proceed without exchange of isospin between the colliding nucleons. Direct excitation of strange isobars can be ruled out. Evidence is presented for reduced probability of isobar production at 0°.

## I. INTRODUCTION

THE experimental data presented in this paper were obtained during a detailed investigation of particle production at small angles. For the first time absolute cross sections for the production of pions, kaons, protons, and antiprotons in proton-proton collisions were obtained at 0°. For an investigation of the dynamics of particle production, data on proton-proton collisions are most relevant. Information on the angular distribution was obtained by repeating the experiment at an angle of 5.7° (100 mrad). The primary momenta were 18.8 and 23.1 GeV/$c$, in some cases also 8.65 and 11.8 GeV/$c$. Data were also taken for collisions of protons with complex nuclei, beryllium and lead; they have mainly practical use for the design of secondary beams. The data on particle production from proton collisions with complex nuclei also gave information on proton-neutron collisions and reabsorption phenomena. In particular, they were of importance for an improved calculation of the neutrino spectrum in the CERN neutrino experiment.[1]) It was for this purpose that this investigation was originally started. In total, more than 300 differential cross sections have been measured.

Previous experimental studies of particle production in nucleon-nucleon collisions, with cosmic rays and accelerators, have established some general characteristics of this process. They will be recalled in the following[2] without giving special reference to individual contributions.

(1) The mean inelasticity in high-energy collisions, defined as the mean fraction of energy going into particle production, remains small throughout the primary energy range 10 to $10^5$ GeV.

(2) The mass spectrum of secondary particles remains approximately the same up to the highest energies studied with cosmic rays. The total energy carried away by pions is a small fraction, about 30% of the primary nucleon energy.

(3) In the center-of-mass system, the longitudinal momentum spectrum of protons is peaked towards the maximum possible momentum, in contrast with the pion spectrum which is peaked at low momenta. The mean energy carried away by the nucleon component is approximately 60% of the initial energy.

(4) The momentum spectrum of pions is characterized by an exponential tail at the high-energy end. As the primary energy $E_0$ is raised, the mean kinetic center-of-mass energy of pions remains constant, the mean pion multiplicity increasing roughly as $E_0^{1/4}$.

(5) Pions and kaons are produced with transverse momenta distributed approximately as a Boltzmann law. The average transverse momentum is about 400 MeV/$c$ and remains constant up to cosmic-ray energies. There is some evidence that the baryonic component has a similar distribution of transverse momentum, but the average transverse momentum seems to increase slightly with the mass of the baryon.

† A first account of this work was presented at the International Conference on Elementary Particles, Siena 1963.

*Now at Deutsches Elektronen Synchrotron, Hamburg, Germany.

[1] G. Bernardini, G. von Dardel, P. Egh, H. Faissner, and F. Terrero, *Proceedings of the Siena International Conference on Elementary Particles 1963*, edited by G. Bernardini and G. P. Puppi (Societa Italiana di Fisica, Bologna, 1963). Vol. I, p. 571.

[2] See, for example, for a review up to 1958: D. H. Perkins, in *Progress in Cosmic Ray and Elementary Particle Physics* (North-Holland Publishing Company, Amsterdam, 1960), Vol. 5.

Several models were proposed (statistical model,[3,4] fireball model,[5] one-pion exchange model,[6] multiperipheral model,[7] etc.) to account for these general characteristics. They either reproduce some average features, such as the center-of-mass energy spectra, averaged over all angles (statistical model), or some dynamical features, such as the angular distribution (peripheral model). The best description is obtained by a set of empirical rules[8] as suggested by the data.

Some finer details of the experimental data about the dynamics of particle production have however been left out in this list of general characteristics.

At low primary momenta of a few GeV/$c$, the process of pion production has been successfully described by the isobar model of Lindenbaum and Sternheimer.[9] However, no information about the angular distribution of isobar formation was yet available. More recent data[10] on pion production in proton-proton collisions at 2.9 GeV gave satisfactory agreement both with the isobar model,[9] using an explicit expression for the angular distribution of isobar formation, and with the one-pion exchange model.[6] Detailed calculations, using an explicit mechanism for exciting the incident as well as the target nucleon through one pion exchange, gave quantitative agreement with experimental data[11] on the angular distribution of isobar formation for small momentum transfers, $|t|<6m_\pi^2$.

At the highest accelerator energies there is also experimental evidence from near elastic proton scattering for the excitation of the nucleons.[12] However, the exchange phenomena leading to this isobar excitation were found to be drastically different. The angular distribution of isobar excitation was observed to follow the diffraction pattern of elastic proton-proton scattering, up to momentum transfers which are far outside the range of validity of the one-pion exchange model. Moreover, the excitation of the first isobar with isospin $I=\frac{3}{2}$ was observed[12a] to disappear very rapidly as the primary energy was increased; at the highest accelerator energies, only excitation of isobars with isospin $I=\frac{1}{2}$ was observed experimentally. This difference in isobar excitation at low and high primary energies was attributed to the vanishing of inelastic contributions with exchange of one unit of isospin (such as the one-pion exchange), and the increasing importance of processes without exchange of isospin.[13]

In the following, we shall try to investigate the role of isobar excitation in the production of secondary particles at the highest accelerator energies. We are following here a model proposed by Peters.[14] Particles emitted in the decay of isobars may be distinguished by the high velocity of the parent isobar in the laboratory system. In the decay to the ground state by single-pion emission, the mean total energy retained by the pion in the isobar rest frame is

$$(M_B^2-M_p^2+m_\pi^2)/2M_B,$$

where $M_B$ is the isobar mass. For an average mass of $M_B=1.6$ GeV, each isobar will, on the average, transfer 30% of its energy to one, or sometimes two pions. As a consequence of the velocity of their parent isobar, decay pions can carry a large fraction of the primary momentum. The average fraction is determined by the isobar mass and by the angular distribution of isobar formation and is approximately independent of the primary momentum. As a consequence of this, the average secondary momentum of decay pions will scale linearly with the primary momentum.

The kinetic energy remaining in the collision rest system (defined as the over-all center-of-mass system) as the colliding nucleons go on in an excited state will also contribute to secondary-particle production. This process will produce the bulk of secondaries observed at large angles. The average momentum in the collision rest system $\langle\bar{p}\rangle$ is known to be small and constant, independent of the primary momentum. In the laboratory system this contribution is characterized by small secondary momenta, of the order of $\langle\bar{p}\rangle\bar{\gamma}c$, where $\bar{\gamma}c$ is the Lorentz factor of the c.m. system, scaling roughly as the square root of the primary momentum. These kinematical differences will be useful in the discussion of the experimental results.

In the following section the experimental setup is described. The main qualitative features of the experi-

[3] E. Fermi, Progr. Theoret. Phys. (Kyoto) **5**, 570 (1950).
[4] R. Hagedorn, Nuovo Cimento **15**, 434 (1960).
[5] P. Ciok, J. Gierula, R. Holynski, A. Jurak, M. Miesowicz, T. Saniewska, O. Stanic, and J. Pernegr, Nuovo Cimento **8**, 166 (1958); G. Cocconi, Phys. Rev. **111**, 1699 (1958).
[6] G. F. Chew and F. E. Low, Phys. Rev. **113**, 1640 (1959); F. Selleri, Phys. Rev. Letters **6**, 64 (1961); E. Ferrari and F. Selleri, Nuovo Cimento **27**, 1450 (1963); E. Ferrari, *ibid.* **30**, 240 (1963).
[7] D. Amati, S. Fubini, A. Stanghellini, and M. Tonin, Nuovo Cimento **22**, 569 (1961).
[8] G. Cocconi, L. J. Koester, and D. H. Perkins, University of California Radiation Laboratory Report No. UCRL SS-28-2, 1961 (unpublished).
[9] S. J. Lindenbaum and R. M. Sternheimer, Phys. Rev. **105**, 1874 (1957); R. M. Sternheimer and S. J. Lindenbaum, *ibid.* **123**, 333 (1961).
[10] A. C. Mellissinos, T. Yamanouchi, G. G. Fazio, S. J. Lindenbaum, and L. C. L. Yuan, Phys. Rev. **128**, 2373 (1962).
[11] G. B. Chadwick, G. B. Collins, P. J. Duke, T. Fujii, N. C. Hien, M. A. R. Kemp, and F. Turkot, Phys. Rev. **128**, 1823 (1962).
[12] A. N. Diddens, E. Lillethun, G. Manning, A. E. Taylor, T. G. Walker, and A. M. Wetherell, *Proceedings of the 1962 Annual International Conference on High-Energy Physics at CERN* edited by J. Prentki (CERN, Geneva, 1962), p. 576; G. Cocconi, A. N. Diddens, E. Lillethun, G. Manning, A. E. Taylor, T. G. Walker, and A. M. Wetherell, Phys. Rev. Letters **87**, 450 (1961); G. Cocconi, E. Lillethun, J. P. Scanlon, C. A. Stahlbrandt, C. C. Ting, J. Walters, and A. M. Wetherell, Phys. Letters **8**, 134 (1964).
[12a] G. Cocconi, E. Lillethun, J. P. Scanlon, C. A. Stahlbrandt, C. C. Ting, J. Walkers, and A. M. Wetherell, Phys. Letters **8**, 134 (1964).
[13] D. Amati, L. L. Foldy, A. Stanghellini, and L. Van Hove, Nuovo Cimento (to be published).
[14] B. Peters, *Proceedings of the 1962 Annual International Conference on High-Energy Physics at CERN*, edited by J. Prentki (CERN, Geneva, 1962), p. 623; Yash Pal, B. Peters, Kgl. Danske Videnskab. Selskab, Mat. Fys. Medd. **33**, No. 15 (1964).

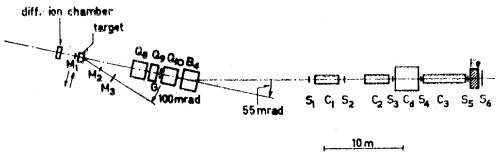


FIG. 1. Experimental layout of the spectrometer and the counter telescope. $M_{1-3}$, monitor; $Q_8$–$Q_{10}$, quadrupole lenses; $B_4$, bending magnet; $G$, guard counters; $S_1$–$S_6$, scintillators; $C_1$–$C_3$, threshold Čerenkov counters; $C_d$, differential Čerenkov counter; Fe, 1 m iron absorber.

mental data will be discussed in Sec. III, with special reference to the role of isobar excitation. Finally, in Sec. IV, the observations on the experimental data from Sec. III will be summarized and their consistency will be discussed.

In the Appendix, all differential cross sections obtained during this experiment are presented in Tables III-XI.

## II. EXPERIMENTAL METHOD

Targets were placed in the focus of a scattered-out proton beam of the CERN proton synchrotron, containing some $10^7$ protons per burst in an image 2 cm wide by 3 cm high, with a momentum band of $\pm 1\%$ and a divergence of $\pm 3$ mrad. The number of protons hitting the target was monitored by a counter telescope $M_2M_3$ (Fig. 1), looking at secondaries which leave the target at a mean angle of 100 mrad; it was calibrated using in coincidence a small scintillator $M_1$ placed in front of the target. This calibration was found to be reproducible to within $\pm 3\%$.[15] A differential ion chamber,[16] placed in front of the target, monitored the position of the proton beam.

Secondary particles produced in the target were analyzed in momentum and brought to a focus on counter $S_5$ by a spectrometer consisting of a quadrupole triplet $Q_8Q_9Q_{10}$ and a bending magnet $B_4$; in the 0 mrad position, the bending magnet separated secondaries from the incident proton beam, giving a spatial separation at counter $S_1$ of 25 to 70 cm for positive particles and more for negative particles. In the 100 mrad measurements, the whole setup was rotated around the target; the incident proton beam then cleared the spectrometer completely.

Secondaries were then defined in direction by the counter telescope $S_1$ to $S_5$ and identified by the Čerenkov counters $C_1C_2C_3$[17] (threshold) and $C_d$ (differential).[18] Using appropriate combinations of the signals of these counters, all particles of the same charge ($\pi^+$, $K^+$, $p$ or $\pi^-$, $K^-$, $\bar{p}$) were identified simultaneously. A large scintillator $S_6$ placed behind 1 m of iron, was used to reject muons by anticoincidence.

Severe experimental problems arise in the 0 mrad measurements from the fact that the proton beam traverses the spectrometer together with secondaries produced in the target. Table I depicts the situation in two typical cases in which the spectrometer is set for 10 GeV/$c$ secondaries of positive and negative charge at 18.8 GeV/$c$ primary momentum.

TABLE I. Number of particles traversing the spectrometer (per burst).

| | | | |
|---|---|---|---|
| Protons of the incident beam: $2\times10^7$ | 70 $\pi^+$ | 8 $K^+$ | 400 $p$ |
| | 35 $\pi^-$ | 0.35 $K^-$ | 0.04 $\bar{p}$ |

Unwanted secondaries may be produced by protons of the incident beam hitting the pole pieces of the spectrometer; the protons producing these interactions come from the halo surrounding the incident beam. There is also a finite probability for any proton of the incident beam to be scattered into the counter telescope, giving rise to false proton or false kaon counts; one should notice here that the $\beta$ of 10 GeV/$c$ kaons is roughly equal to that of 18 GeV/$c$ protons. Both these effects result in a counting rate without target which is a significant fraction of that with target; moreover, the effect is target-dependent because the number of protons through the spectrometer is reduced when the target is in position.

The following precautions helped to improve this situation:

(1) Thin targets were used to avoid excessive blowing up of the proton beam by multiple scattering.

(2) Multiple and nuclear scattering from the air throughout the spectrometer was minimized by inserting He bags.

(3) All secondaries produced in the pole pieces of the spectrometer and liable to reach the countertelescope were vetoed by *guard counters* placed inside the spectrometer. They also served to define a simple diaphragm for particles produced in the target which greatly simplified a reliable calculation of the solid angle.

(4) The high counting rate of the guard counters gave rise to losses due to accidental anticoincidences. These were therefore continuously monitored and used for correcting the data. This effect was always smaller than 10%.

The measured cross sections for production of $\pi^\pm$, $K^\pm$, $p$, and $\bar{p}$, at 0 and 100 mrad from $p$–$p$, $p$–Be and $p$–Pb interactions at 18.8 and 23.1 GeV/$c$ are given in the Appendix, Tables III-VIII; some cross sections for pion and proton production at 0° obtained in $p$–Be collisions at 8.65 and 11.8 GeV/$c$ primary momentum are

[15] The neutron contamination was found to be smaller than 1%.
[16] A. J. Metheringham and T. R. Willitts, Nucl. Instr. Methods **15**, 297 (1962).
[17] M. Vivargent, G. von Dardel, R. Mermod, G. Weber, and K. Winter, Nucl. Instr. Methods **22**, 165 (1963).
[18] R. Mermod, K. Winter, G. Weber, and G. von Dardel, *Proceedings of an International Conference on Instrumentation for High-Energy Physics, Berkeley 1960* (Interscience Publishers, Inc., New York, 1961), p. 172.

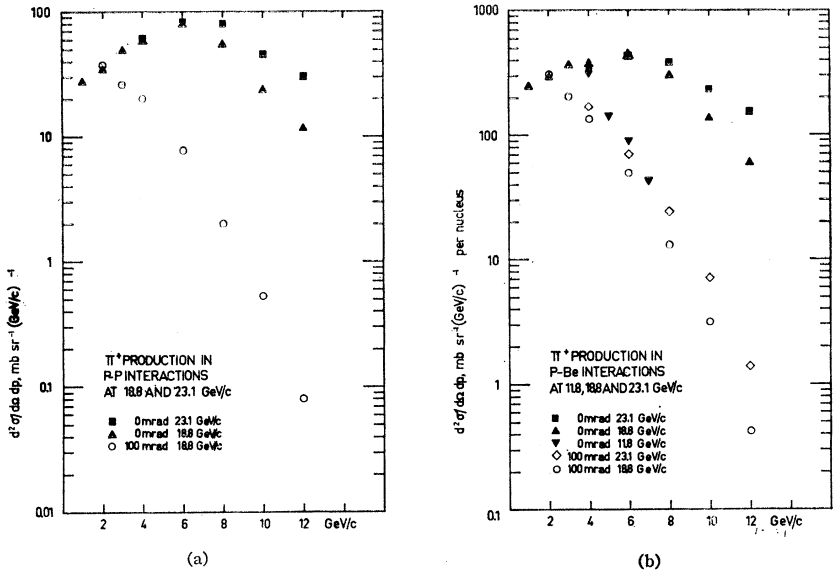


FIG. 2. Momentum spectra of positive pions at 0 and 100 mrad, for primary momenta of 18.8 and 23.1 GeV/$c$, as observed in (a) $p$–$p$ collisions, (b) $p$–Be collisions.

given in the Appendix in Tables IX-XI each table corresponding to one particle of given charge. The cross sections are expressed in mb sr$^{-1}$ (GeV/$c$)$^{-1}$ per nucleus and not in number of secondaries per interaction; this would have implied the use of the total cross section, which is not accurately known, for nuclei.

Corrections have been applied for particle decay, for accidental coincidences, for absorption, multiple scattering and diffraction scattering in the target and the telescope and for differential Čerenkov counter efficiency. The errors quoted include both statistical and systematical uncertainties; the latter arise from approximations in the computation of the corrections as well as from the uncertainty in the intensity of the incident beam. Error bars are shown in figures for $K^{\pm}$ and $\bar{p}$; errors on $\pi^{\pm}$ and $p$ are of the same order as the size of the points.

Absorption corrections are important as the simultaneous identification of three kinds of particles requires several counters and consequently introduces a certain amount of material in the path of the secondaries. $K$ and $\bar{p}$-nucleus absorption cross sections are often not available and have been computed from cross sections on hydrogen with the help of a semiempirical formula derived by Williams,[19] which is more accurate than the "geometrical" formula $\sigma=\sigma_0 A^{2/3}$. Typical corrections are of the order of 20% for 6 GeV/$c$ positive pions.

No simple evaluation of losses by multiple scattering can be done when the scatterer is extended, as in the case of our counter telescope; consequently, a Monte-Carlo calculation was done. This considers both the particles which are scattered out of the telescope and those which would leave the telescope but are scattered back into it, taking into account the spatial distribution of the beam, which was not uniform in our case because of the focusing action of the lenses. Typically, corrections are smaller than 10% for 6 GeV/$c$ secondaries.

The problem of losses by diffraction scattering is similar; minor modifications to the computer program allowed the calculation of the fraction of diffraction scattered secondaries which are lost for the telescope, yielding a typical correction of 5% for 6 GeV/$c$ positive pions.

The effect of the finite average angular acceptance of $\pm 8$ mrad on the 0 mrad data has been investigated. Extrapolation to zero solid angle requires assumptions on the detailed shape of the angular distribution. This is strongly momentum-dependent. An upper limit for this correction was estimated with the help of the empirical formula given by Cocconi, Koester, and Perkins,[8] which overestimates this effect. These limiting corrections varied from less than 1% to less than 10% for 1 and 12 GeV/$c$ secondaries, respectively, and were neglected.

## III. EXPERIMENTAL RESULTS

### 1. Pion Spectra

The differential momentum spectra of positive and negative pions observed at 0 and 100 mrad in the laboratory system, for different primary momenta and targets are presented in Figs. 2 and 3.

Inspection of these spectra and a comparison with other data, on negative pion production in proton-beryllium collisions in the angular range 25–125 mrad[20] and on neutral pion production in proton-proton colli-

[19] R. W. Williams, University of Washington, Seattle (unpublished).

[20] A. N. Diddens, E. Lillethun, G. Manning, A. E. Taylor, T. G. Walker and A. M. Wetherell (private communication).

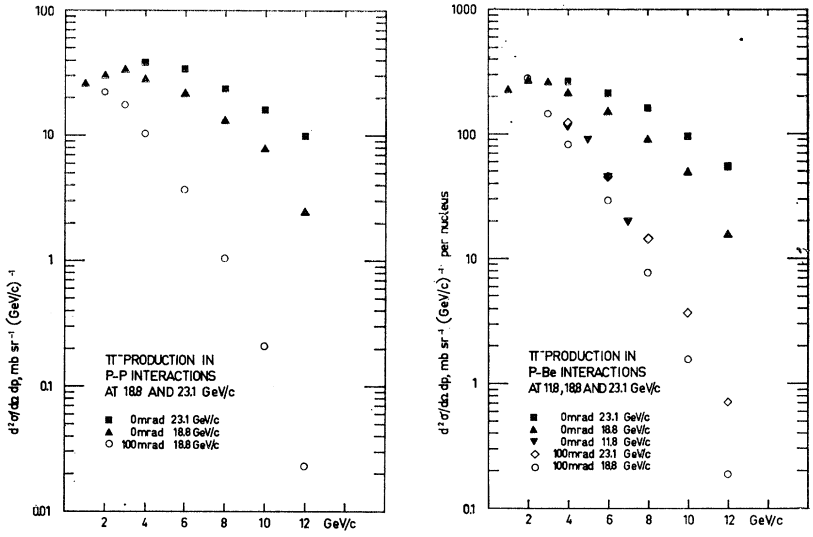


FIG. 3. Momentum spectra of negative pions at 0 and 100 mrad, for primary momenta of 18.8 and 23.1 GeV/$c$, as observed in (a) $p$–$p$ collisions, (b) $p$–Be collisions.

sions in the angular range 30–500 mrad[21] leads us to the following general observations:

(i) The differential momentum spectra of positive and negative pions at $0^0$ differ strongly in shape. This is best observed on a linear plot in Fig. 4. The spectrum of positive pions exhibits a pronounced maximum at 6.3 GeV/$c$ for 18.8 GeV/$c$ primary momentum, which is shifted to 6.8 GeV/$c$ for 23.1 GeV/$c$ primary momentum. In contrast to this, a smooth spectrum is observed for negative pions; only the high-momentum tail is observed to shift linearly with the primary momentum.

(ii) At small angles, the cross section for production of pions with secondary momenta below 5 GeV/$c$ is approaching a constant value in the laboratory system, independent of the primary momentum.

(iii) At fixed secondary momentum, the production of pions increases strongly as the angle is decreased. However, in the very-small-angle range between 0-25 mrad, and for higher secondary momenta, the production hardly changes.

(iv) There is experimental evidence that the production of pions with low secondary momenta is more abundant at small angles than at $0^0$.

These general observations will now be discussed in more detail in connection with the model for particle production which was given in Sec. I.

### *Spectra of Positive and Negative Pions*

The average momentum of pions produced in the decay of isobars by single pion emission will scale linearly with the primary momentum. To arrive at the momentum spectrum for single $\pi^+$ production, we have to use some subtraction technique. It was supposed that in proton-proton collisions, negative and positive pions are produced mainly in the decay of a single isobar of isospin $\frac{1}{2}$. This hypothesis will be justified later in this section. The ratio of positive to negative pions produced in the decay of an isobar of isospin $\frac{1}{2}$ by emission of two pions is 7/5.[9] The momentum spectrum for single $\pi^+$ production at $0^0$ was then obtained by the subtraction

$$(d^2\sigma/d\Omega dp)(0^0,p;\pi^+ \text{ single}) = (d^2\sigma/d\Omega dp)(0^0,p;\pi^+ \text{ exper.}) - (7/5)(d^2\sigma/d\Omega dp)(0^0,p;\pi^- \text{ exp.}).$$

The resulting average momenta of the single $\pi^+$ spectra at $0^0$ are 6.5 and 7.8 GeV/$c$ for 18.8 and 23.1 GeV/$c$ primary momentum, respectively. This result is compatible with the transfer of a constant average fraction of the primary momentum to single decay pions. Neglecting the influence of the angular distribution of isobar formation, we can relate this average fraction to an average isobar mass of 1.64 GeV.

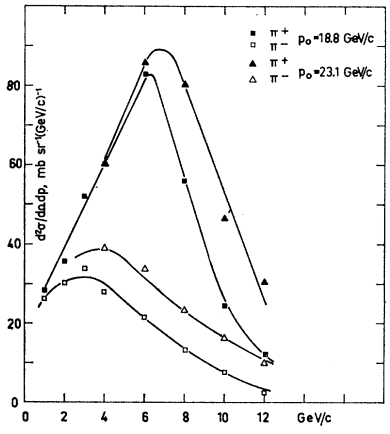


FIG. 4. Comparison of momentum spectra of positive and negative pions observed at 0° in $p$–$p$ collisions with primary momenta of 18.8 and 23.1 GeV/$c$.

[21] M. Fidecaro, G. Finocchiaro, G. Gatti, G. Giacomelli, W. C. Middelkoop, and T. Yamagata, Nuovo Cimento **24**, 73 (1962).

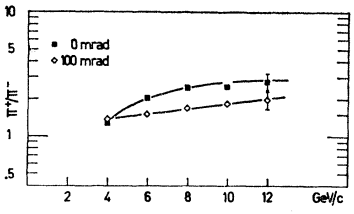


FIG. 5. Ratio $\pi^+/\pi^-$ as a function of secondary momentum at 0 and 100 mrad observed in $p$–Be collisions at 23.1 GeV/$c$.

The maximum fraction of primary momentum which an isobar can transfer to a single pion is about 70% for an isobar mass of 1.68 GeV. This is unfortunately outside the momentum range of this experiment. Observation of a fast, sudden drop in the pion spectrum at high momenta could in fact be used to put a lower limit on the mass of isobars frequently excited in nucleon-nucleon collisions.

The pronounced difference in shape of the spectra observed for positive and negative pions at $0^0$ can also be demonstrated by considering the ratio of positive to negative pions, $N(\pi^+)/N(\pi^-)$. This quantity is shown in Figs. 5 and 6 as a function of secondary momentum for different angles and primary momenta. At low secondary momenta, it is close to one; as the momentum increases, a steep rise is observed and finally a constant value is reached, varying only with the angle. The step in the momentum dependence of the ratio $N(\pi^+)/N(\pi^-)$ is observed to shift approximately linearly with the primary momentum.

Isobar decays into other channels are known to contribute about 20% to the total rate.[22] The contribution from more complicated decays, for instance into two pions,[23] is evidenced by the shift, with primary momentum, of the high-momentum tail in the $\pi^-$ spectrum. In decays into two pions, the average fraction of energy transferred to each pion is about 15%. The maximum observed in the $\pi^-$ spectrum at 18.8 GeV/$c$ primary momentum does indeed occur at about 0.15 $p_0$.

But apparently, few negative pions are produced by single pion decay of isobars. This surprising result implies that the incident nucleon does not change its charge when it is excited, a statement equivalent to the observation that at high primary energies the exchange phenomena responsible for isobar excitation are processes without exchange of isospin.[12,13] This result is further supported by the experimental evidence from our data that the ratio $N(\pi^+)/N(\pi^-)$ is independent of the target nucleus, a result which is to be expected when isobar excitation is proceeding through processes without exchange of isospin.

Further direct evidence against the excitation of isobars with isospin $I=\frac{3}{2}$ is obtained from the ratio of positive to neutral pions at fixed secondary momentum. On the basis of isospin conservation the decay probabilities of a positively charged isobar into $\pi^+$ or $\pi^0$ are in the ratio $N(\pi^+)/N(\pi^0)=2$ for isospin $\frac{1}{2}$, and $\frac{1}{2}$ for isospin $\frac{3}{2}$. A comparison of our data on $\pi^+$ production with other data[21] on $\pi^0$ production at 100 mrad gives a ratio of $1.6\pm0.3$ in the relevant range of secondary momenta (see Fig. 6), compatible with $I=\frac{1}{2}$ but excluding $I=\frac{3}{2}$.

The probability for simultaneous excitation of the incident and of the target nucleon to states of isospin $\frac{3}{2}$ is strongly limited by the observation that the ratio $N(\pi^+)/N(\pi^-)$ is independent of the target nucleus. The ratio of positive to negative pions from the decay of two isobars with isospin $\frac{3}{2}$ is predicted[9] to change by a factor of about 4 between proton-proton and proton-neutron interactions.

This experimental fact of unequal population of the different isospin states could certainly not be understood on the basis of a statistical model. This model, on the contrary, predicts that all isospin and spin states are populated according to their respective statistical weights. The statistical model, however, may be adequate to describe particle production from the kinetic energy remaining in the collision rest system as the colliding nucleons go on in an excited state. It predicts, in fact, the observed constant mean kinetic c.m. energy[4] and gives also excellent agreement with experimental data on the c.m. spectrum, averaged over all angles.[21] This agreement shows that, though pions created by the decay of isobars carry high energy, their number, averaged over all angles, is small as compared to the pion multiplicity in pionization processes.

With this justification in mind, it will be instructive to compare the experimental data at $0^0$, transformed to the c.m. system, with the momentum spectrum predicted by the statistical model.[4] This comparison is shown for positive and negative pions in Fig. 7; the spectrum given by the statistical model is supposed to give a good approximation to particle production in the collision rest system. Fair agreement is found for small momenta where mainly multipion production is contributing. The comparison at high momentum gives an indication of the strong contribution from isobar decays.[9,10] The respective average momenta $\langle\bar{p}\rangle$ are given in Table II, together with data from bubble chamber work[24] on events with charged-pion multiplicities $\geq 4$, averaged over all angles. This comparison shows unam-

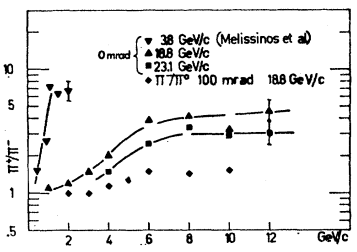


FIG. 6. Ratios $\pi^+/\pi^-$ and $\pi^+/\pi^0$ versus secondary momentum as observed at different primary momenta in $p$–$p$ collisions. Data for $p_0$ $=3.8$ GeV/$c$ are taken from Melissinos *et al.* (Ref. 10).

[22] B. Musgrave, G. Petmezas, L. Riddiford, R. Bock, E. Fett, and B. R. French, Nuovo Cimento (to be published)

[23] The ratio $\pi^+/\pi^-$ expected from the decay of the 1688-MeV isobar is estimated to 3.2 from data given in Ref. 28.

[24] S. J. Goldsack, L. Riddiford, B. Tallini, B. R. French, and W. Neale, Nuovo Cimento **23**, 941 (1962).

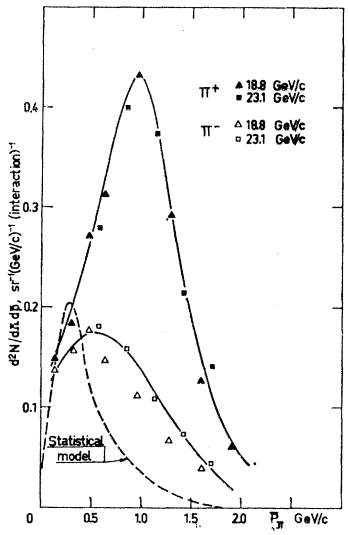


FIG. 7. Momentum spectra of positive and negative pions at 0° for $p$–$p$ collisions at 18.8 and 23.1 GeV/$c$ transformed to the center-of-mass system versus longitudinal c.m. momentum $\bar{p}_L$. The dashed curve gives the prediction of the statistical model (Ref. 4).

biguously the strong contributions from isobar decays to both positive and negative pions at 0°; note, however, the good agreement with the statistical model for high-multiplicity events, averaged over all angles.

TABLE II. Average momenta (in GeV/$c$) in the c.m. system compared to the prediction of the statistical model (Ref. 4) and to experimental results from bubble chamber work (Ref. 24), averaged over all angles.

| | This experiment 0° | Statistical model (Ref. 4) | Bubble chamber (Ref. 24) (averaged over all angles) |
|---|---|---|---|
| $\langle\bar{p}_{\pi^+}\rangle$ | 1.00 | 0.540 | 0.550 |
| $\langle\bar{p}_{\pi^-}\rangle$ | 0.70 | | |

### *Excitation Curves*

Varying the primary momentum, it was observed [see Figs. 8(a) and 8(b)] that the cross section in the laboratory system for production of pions at 0° with secondary momenta below 5 GeV/$c$ tends to approach a constant value. This was in fact predicted by a multiperipheral model.[7] The decoupling from the primary momentum is introduced in this model, by assuming that pion production in the collision rest system takes place by multipion interaction in the exchange process between the colliding nucleons. For secondaries of small momentum a unique laboratory spectrum is predicted which depends on the mass and on the transverse momentum of the secondaries, but not on the primary energy. It would be interesting to search for such a behavior over a wider range of primary and secondary momenta.

### *Angular Distribution at High Secondary Momentum*

The variation of pion production with laboratory angle and secondary momentum has already been investigated by several authors.[25] In the range of angles larger than 5°, it was found that the probability for emission of a pion with secondary momentum $p$ and transverse momentum $p_t = p\sin\Theta$ can be expressed as a product of two probability distributions, $g(p)$ and $f(p_t)$. Using the general characteristics of particle production, as mentioned in Sec. I, Cocconi *et al.*[8] obtained an excellent fit to all data on pion production[26] in the angular range $\Theta > 5°$ with the empirical formula

$$(d^2\sigma/d\Omega dp) = (n_\pi/2\pi)(4p^2/\langle p_t\rangle^2\langle p\rangle) \exp(-p/\langle p\rangle)\exp(-2p_t/\langle p_t\rangle).$$

Here $n_\pi$ is the effective pion multiplicity, $\langle p\rangle$ and $\langle p_t\rangle$ are the mean secondary momentum and the mean transverse momentum, respectively. Typical values obtained for these parameters are $\langle p_t\rangle = 350$ MeV/$c$, $\langle p\rangle = 2$ GeV/$c$. The validity of this empirical rule in the small-angle range can be tested by plotting the ratio of cross sections for pion production at 0 and 100 mrad against secondary momentum. The empirical rule predicts this ratio to be given by the expression

$$\exp(2p\Theta/\langle p_t\rangle).$$

The experimental data are shown in Fig. 9; the solid lines give the prediction of the empirical rule for different average transverse momenta. The plotted ratio is

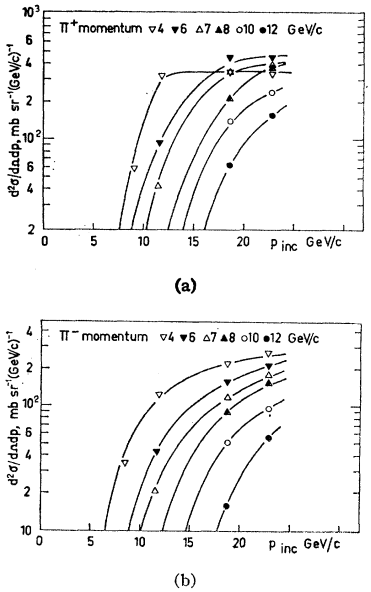


FIG. 8. (a) Production of positive pions at 0° in $p$–Be collisions at fixed secondary momentum for primary momenta of 8.65, 11.8, 18.8, and 23.1 GeV/$c$. (b) Production of negative pions at 0° in $p$–Be collisions for different primary momenta.

[25] See, for complete list of references, D. R. O. Morrison, CERN Internal Report, CERN/TC/Physics 63-1 (unpublished).
[26] W. F. Baker, R. C. Cool, E. W. Jenkins, T. F. Kycia, and S. J. Lindenbaum, Phys. Rev. Letters 7, 101 (1961).

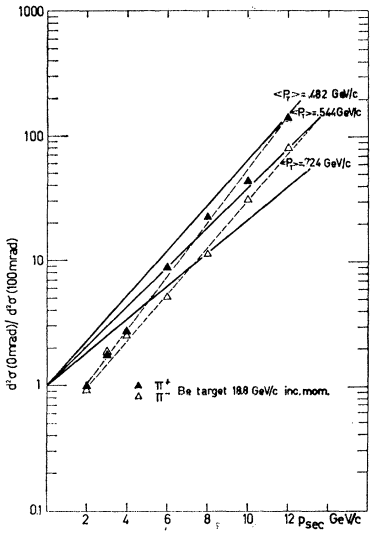


FIG. 9. Angular distribution of positive and negative pions in $p$–Be collisions at 18.8 GeV/$c$. Plotted is the ratio of cross sections at 0 and 100 mrad versus secondary momentum.

seen to follow an exponential with a slope of $\langle p_t \rangle = 0.40$ GeV/$c$ for positive pions and $\langle p_t \rangle = 0.46$ for negative pions, respectively, in good agreement with data at larger angles. However, a ratio equal to one, predicted by the empirical rule for zero secondary momentum, is observed to occur at a momentum of about 2 GeV/$c$; extrapolating to zero momentum gives a ratio of 0.4 for positive pions and of 0.5 for negative pions. Since a good fit of the data for angles $\Theta > 5^0$ was obtained with this rule, as mentioned before, we conclude that for angles close to $0^0$ the production of pions of both polarities is increasing less rapidly with decreasing transverse momentum. To investigate this apparent suppression of pion production at $0^0$ further, a comparison with other data, at angles between 25 and 30 mrad has been done. The high-momentum tail of the $\pi^+$ spectrum at $0^0$ has been compared to data on $\pi^0$ production in proton-proton collisions.[21] In making this comparison, one should keep in mind that both positive and neutral pions of high secondary momentum, $p_\pi \geq 6$ GeV/$c$, are supposed to emerge from the decay of positively charged isobars of isospin $\frac{1}{2}$. Consequently, the expected ratio $N(\pi^+)/N(\pi^0) = 2$ has been taken into account in Fig. 10. One notices that the production in the secondary-momentum range considered is hardly changing between 0 and 30 mrad. Remembering the finite angular acceptance of $\pm 8$ mrad in this experiment, an actual dip in the angular distribution at $0^0$ cannot be excluded. A similar conclusion is reached for the high-momentum tail of negative pion production at $0^0$, as compared to unpublished data at 25 mrad.[20]

Considering now the angular distribution of parent isobars, one could in principle, using some information on the different partial waves contributing to the decay of different isobars, deduce it by unfolding the observed angular distribution of decay pions. In practice this analysis would only be significant if the probabilities of exciting different isobars, decaying into different partial waves were known. We can, however, arrive at the more qualitative conclusion that the probability for exciting the incident nucleon is reduced when the angle is not changed during the collision. Some more quantitative statements will be given later, from an analysis of the proton momentum spectrum at $0^0$. A suppression of isobar excitation at small angles as compared to elastic scattering has in fact already been observed in experiments on near-elastic scattering of protons.[12]

Isobars are known to have high spin values which increase with increasing mass. Classically, the change in orbital angular momentum without change in direction is related to the change in momentum in the c.m. system before and after the excitation. Quantum mechanically this means that the probability for changing the orbital angular momentum by one or more units is reduced if the direction is not changed in the collision.

### *Angular Distribution at Low Momenta*

The observation of more abundant production of pions of small secondary momentum at finite angles as compared to $0^0$ (see Fig. 10) may direct this discussion to consider the dependence on the impact parameter of the amount of kinetic energy remaining available for particle production in the collision rest system when the colliding nucleons fly away in an excited state. The angular distribution of excited nucleons was found[12] to be characterized by an exponential decrease of the differential cross section with increasing (four-momentum transfer)$^2 = t$, $\exp(-b|t|)$. At small angles close to $0^0$ the collision is dominated by isobar excitation in two-body reactions. The kinetic energy remaining in the collision rest system is in the statistical average necessarily small and its contribution to pion production at $0^0$ vanishes as compared to isobar decay. As the angle is increased, the probability for the incident nucleons to separate from the collision rest system in an excited state de-

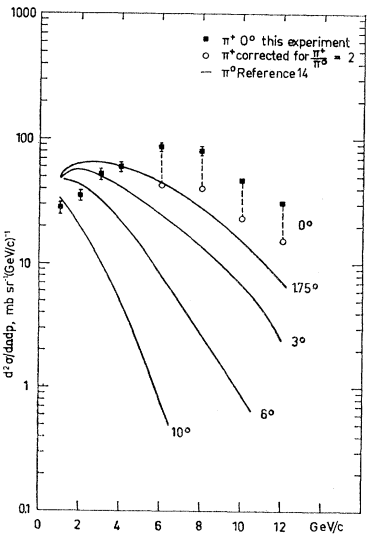


FIG. 10. Comparison of momentum spectra of positive and neutral pions in $p$–$p$ collisions at small angles. Data on $\pi^0$ production are from M. Fidecaro *et al.* (Ref. 21). The cross sections for $\pi^+$ production are shown also taking into account a ratio $\pi^+/\pi^0 = 2$, expected from the decay of a positive isobar of isospin $\frac{1}{2}$.

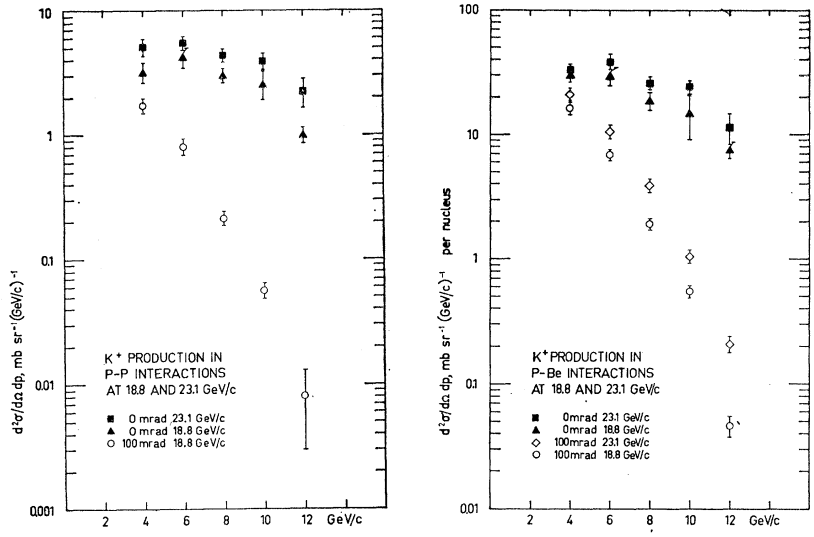


FIG. 11. Momentum spectra of positive kaons at 0 and 100 mrad, for primary momenta of 18.8 and 23.1 GeV/$c$, as observed in (a) $p$–$p$ collisions, (b) $p$–Be collisions.

creases rapidly. Consequently, the kinetic energy remaining available for particle production in the c.m. system will, in the statistical average, increase with decreasing impact parameter and its contribution to pion production will grow. This effect is apparently observed in the low-momentum region of pion spectra at small angles as compared to 0°, most strikingly in Fig. 10, where production of $\pi^+$ at 0° and $\pi^0$ at small angles is compared.

Using the arguments given in the preceding paragraph, the relative numbers of pions at 0° produced in the collision rest system and by isobar decay, are estimated from Fig. 7, to $\frac{1}{3}$, their relative total-energy content in the over-all c.m. system to $\frac{1}{8}$, respectively.

## 2. Kaon Spectra

Production of positive kaons at small angles (Fig. 11) is characterized by a striking similarity with the spectra of positive pions. This is observed most directly in Fig. 12, showing the ratio $K^+/\pi^+$ as a function of secondary momentum for 0 and 100 mrad. One notices that this ratio is constant, close to 10%, independent of angle and primary momentum. Consequently, we consider that the conclusions reached for production of positive pions apply to the production of positive kaons as well; in particular, that there is a high probability of exciting the incident nucleon in a near elastic collision with decay by the emission of a single positive kaon.

Before entering into a discussion of the probability of isobar decay into kaon and hyperon, a few remarks about the data on negative kaon production will be given. This is characterized by a strong dependence on secondary momentum, both at 0 and 100 mrad (Fig. 13) and by the strong dependence on primary momentum. These characteristics of $K^-$ production are seen to be in contrast with the observations for negative pions, as is evidenced by the ratio $K^-/\pi^-$, shown in Fig. 14, as a function of secondary momentum. The production of $K^-$ seems to be dominated by phase space, whereas most negative pions of high momentum are produced in decays of isobars by emission of two pions. This conclusion is supported further by a comparison of the momentum spectrum at 0°, transformed to the c.m. system, with the prediction of the statistical model; the shapes of both spectra are observed to be very similar.

With this conclusion in mind, the possibility of exciting a strange isobar in a near elastic nucleon-nucleon collision may be investigated.[14] Strange isobars, such as the $Y_0^*$ (1520 MeV) and $Y_0^*$ (1815 MeV), for instance, are known to decay to the nucleon ground state by the emission of a single $K^-$, with a probability of 30 and 60%, respectively.[27] The average fraction of energy transferred to a decay kaon would be 36 and 40%, respectively. No peak in the $K^-$ spectrum at secondary momenta around $0.4\times p_0$ has been found at 0°. We therefore conclude that the excitation of strange isobars, requiring an exchange of strangeness between the collid-

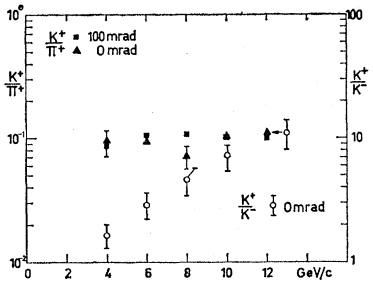


FIG. 12. Observed ratio $K^+/\pi^+$ at 0 and 100 mrad and $K^+/K^-$ at 0 mrad in $p$–Be collisions at 23.1 GeV/$c$.

[27] A. H. Rosenfeld, University of California Radiation Laboratory Report No. UCRL 8030 Rev., 1963 (unpublished).

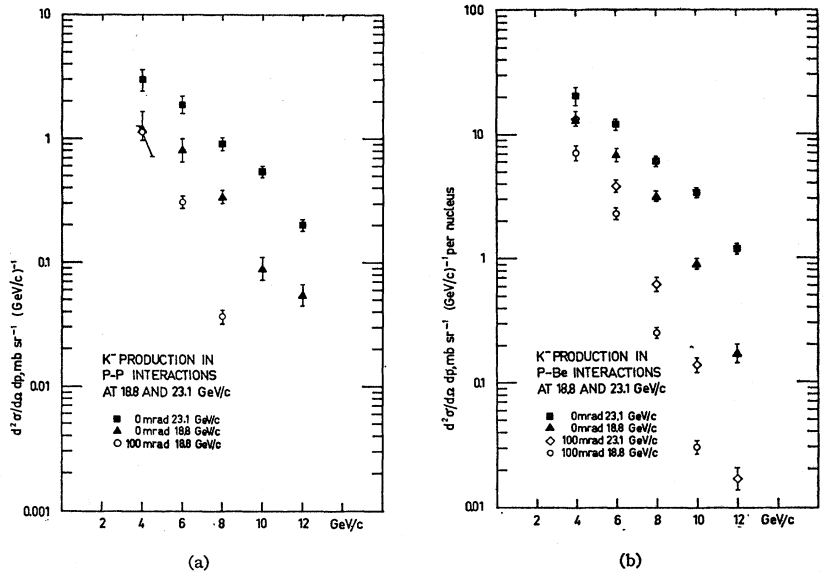


FIG. 13. Momentum spectra of negitive kaons at 0 and 100 mrad, for primary momenta of 18.8 and 23.1 GeV/$c$, as observed in (a) $p$–$p$ collisions, (b) $p$–Be collisions.

ing nucleons, is very improbable as compared to nonstrange isobars.

This can also be demonstrated by the production ratio $K^+/K^-$. If a strange isobar were excited directly in a near elastic collision, with exchange of strangeness between the colliding nucleons, a $K^+$ would have to be produced simultaneously at the other nucleon. Strong excitation of strange isobars would thus tend to give a ratio $(K^+/K^-)\cong 1$, averaged over all momenta. Experimentally, however, this ratio is observed to be larger than one and to increase strongly with increasing secondary momentum, roughly as an exponential (see Fig. 12).

We are now prepared to discuss the probability of nonstrange isobar decay into kaon and hyperon. The isobar $N^*_{1/2\,5/2}$ of mass 1688 MeV is known[22] to decay to $K^+\Lambda_0$ ($d$ wave); the probability with respect to the decay to $\pi^+ n$ has been estimated[28] to be 3%. Assuming that all positive pions of high momentum are emitted in the decay of the two isobars $N^*_{1/2\,3/2}$ (1512 MeV) and $N^*_{1/2\,5/2}$ (1688 MeV), which are known to be excited with about equal probability,[12] we would expect a ratio $K^+/\pi^+\cong 1.5\%$. It is, however, necessary to take into account the respective momenta of the pion and kaon in the isobar rest system and to correct the decay probability by the Jacobian, which for small angles is equal to

$$(p^*_\pi/P^*_K)^2=6,$$

to arrive at the ratio $K^+/\pi^+$ as observed in the laboratory system per fixed element of solid angle and per unit momentum interval. Using this correction, we in fact arrive with the given decay probability, at the observed ratio of 10%.

As a consequence of the smaller momentum of $K^+$ in the isobar rest system, the angular distribution in the laboratory will be more peaked forward. Thus, the suppresion of production at 0°, due to the reduced probability of isobar excitation in the forward direction, should

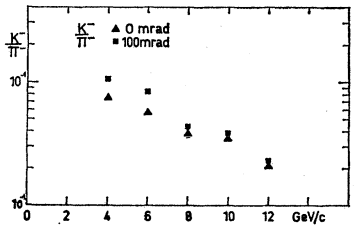


FIG. 14. Ratio $K^-/\pi^-$ observed at 0 and 100 mrad in $p$–Be collisions at 23.1 GeV/$c$.

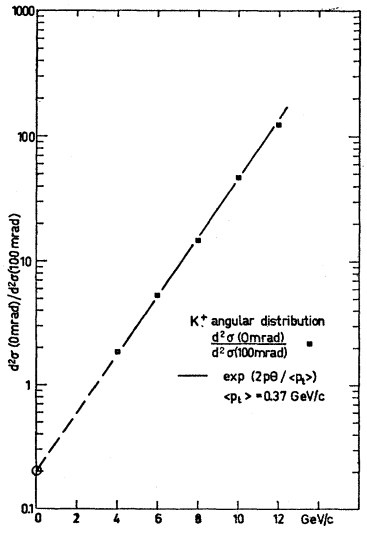


FIG. 15. Angular distribution of positive kaons produced in $p$–$p$ collisions at 18.8 GeV/$c$. Plotted is the ratio of cross sections at 0 and 100 mrad versus secondary momentum. The solid curve is a fit with $a\exp(2p\Theta/\langle p_t\rangle)$ using $a=0.2$, $\langle p_t\rangle=0.37$ GeV/$c$.

[28] J. A. Anderson, F. S. Crawford, B. B. Crawford, R. L. Golden, and L. J. Lloyd, *Proceedings of the 1962 International Conference on High-Energy Physics at CERN* (CERN, Geneva, 1962), p. 271; P. Falk-Vairant and G. Valladas, Rev. Mod. Phys. **33**, 362 (1961).

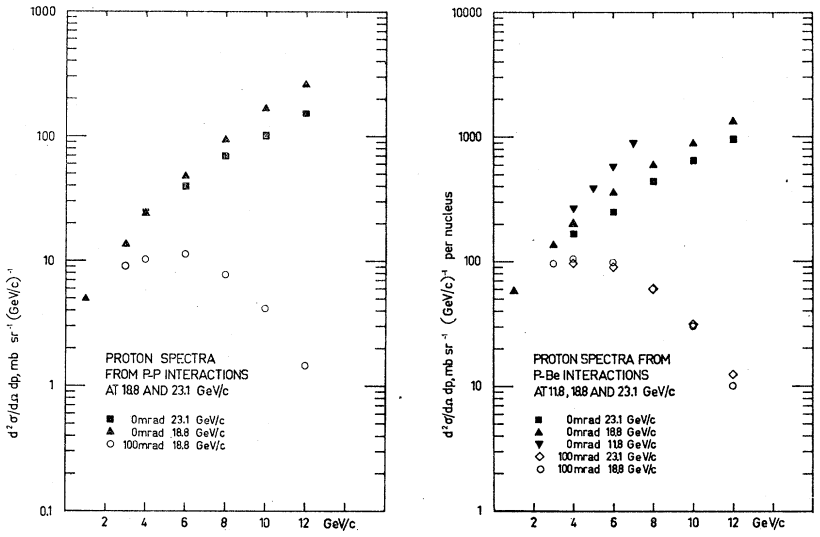


FIG. 16. Momentum spectra of protons at 0 and 100 mrad, for primary momenta of 18.8 and 23.1 GeV/$c$, as observed in (a) $p$–$p$ collisions, (b) $p$–Be collisions.

be more marked for kaons as compared to pions. This can be observed in Fig. 15, showing the ratio of $K^+$ production at 0 and 100 mrad, as a function of secondary momentum. The data are well fitted by an exponential

$$a \exp(2p\Theta/\langle p_t \rangle),$$

using a value of $\langle p_t \rangle = 0.37$ GeV/$c$ for the average transverse momentum. Extrapolation to zero secondary momentum gives $a=0.2$ demonstrating the suppression of $K^+$ production at $0^0$, as compared to 100 mrad, by a factor of 5. The production of $\pi^+$ at $0^0$ was found to be suppressed by a factor 2.5. This consistent observation then helps to increase the confidence in our conclusion about abundant production of positive kaons and pions from the decay of isobars with isospin $\frac{1}{2}$.

### 3. Proton Spectra

Unlike pions and kaons, protons observed at small angles are not "produced" in the proper sense of the word; they are identical to the incident protons and have lost a certain fraction of their primary energy which went into proper production phenomena.

This is strongly exhibited in the momentum spectrum at $0^0$ (Fig. 16), which is observed to increase as an exponential with increasing secondary momentum and to be peaked towards the maximum possible momentum, as already found previously in bubble chamber investigations.[29] It was the observation of this behavior which first stimulated the discussion of particular processes of particle production in which the nucleon retains a large fraction of its primary momentum. To come to more quantitative statements, let us consider a diagram in the c.m. system where the longitudinal momentum $\bar{p}_L$, of an event is plotted against the transverse momentum $p_t$. Each event is represented by the end point of its total momentum vector. A projection of the density distribution in this diagram on the axis $p_t$ and $\bar{p}_L$ gives the probability distribution of these variables. These distributions have been assumed to be independent of each other in a previous analysis[8] of experimental data[26] obtained at laboratory angles $\Theta \geq 5^0$. Using this assumption, good agreement for pion production and for proton fluxes was obtained.

In the forward direction the transverse momentum is zero and a transformation of the observed momentum spectrum to the c.m. system gives directly the probability distribution in longitudinal momentum $\bar{p}_L$. This

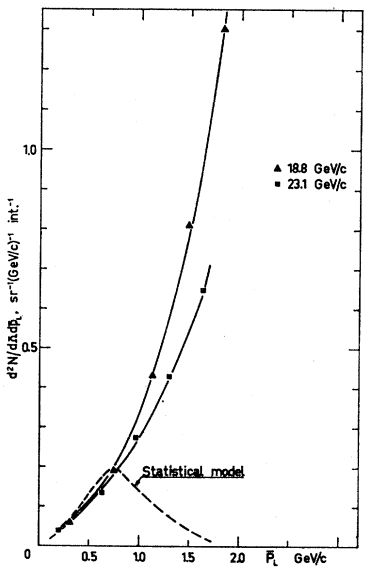


FIG. 17. Probability distribution in longitudinal c.m. momentum $\bar{p}_L$ per steradian of protons observed at 0° in $p$–$p$ collisions at 18.8 and 23.1 GeV/$c$. Also shown is the distribution predicted by the statistical model[4] for central collisions.

[29] D. R. O. Morrison, *Aix-en-Provence Conference on High-Energy Physics 1961*, edited by E. Cremieu-Alcan, P. Falk-Vairant, and O. Lebey (Centre d'Etudes Nucleaires de Saclay, Seine et Oise, 1961), Vol. 1, p. 407.

distribution, expressed as the probability per steradian, GeV/$c$, and interaction is shown in Fig. 17. The high-momentum part is well approximated by an exponential, peaked towards $\bar{p}_0$, the primary c.m. momentum. As the primary momentum is increased, the probability for fixed $\bar{p}_L$ decreases. This effect is in agreement with a constant total area under the distribution; the number of protons per steradian and interaction at 0° remains constant, i.e., the probability of near elastic charge exchange is independent of the primary momentum. This number of protons at 0° per steradian and interaction is also found to be independent of the target nucleus, to within 20%. These observations may be taken as the most convincing confirmation of our preceding conclusion, reached in the discussion of pion and kaon spectra, that only isobars with isospin $\frac{1}{2}$ are excited with high probability in high-energy nucleon-nucleon collisions.

The proton momentum spectrum observed at 0° can be related to the angular distribution of parent isobars. Neglecting the variation of isobar momentum with production angle in the relevant angular range 0-40 mrad, one notices that a unique relation exists between the momentum of a proton observed at 0° and the production angle of its parent isobar. For example, in the decay of an isobar with a mass of 1.6 GeV, produced at 0° and at a primary momentum of 18.8 GeV/$c$, only protons of 6.5 and 18.7 GeV/$c$ are contributed to the momentum spectrum of protons observed at 0° (in the case of infinite angular resolution). Taking into account the Jacobian of the transformation from the isobar rest system to the laboratory system and the finite angular resolution in the experiment, the observed momentum spectrum at 0° can be used to put some limits on the angular distribution of parent isobars.

If the angular distribution of isobar formation were peaked at 0°, following an exponential in $t$= (four-momentum transfer)$^2$ with the slope observed at larger angles,[12] the resulting momentum spectrum of protons at 0° would decrease by a factor of 8 between 7 and 12 GeV/$c$. For an assumed isotropic angular distribution of isobars at small angles, the resulting proton momentum spectrum at 0° would increase by a factor of 1.2 between 7 and 12 GeV/$c$. Experimentally, we find an increase by a factor of 5 between 7 and 12 GeV/$c$. We have therefore to conclude that the observed increase with secondary momentum in the proton spectrum at 0° reflects an increasing isobar production with increasing angle near 0°.

In the light of our conclusion about the importance of isobar excitation and decay in the production of particles, the unique distribution of transverse momentum, according to a Boltzmann law observed for pions and kaons at all angles, including the very small angle range, appears to be the result of a strange accident, produced by the combined action of dynamics, in the production of isobars and of kinematics in their decay. In fact, in the case of protons this accident does not occur.

Figure 18 shows the plot of the ratio of protons observed at 0 and 100 mrad against secondary momentum. The slope of the momentum dependence is observed to increase with increasing momentum. For secondary momenta $p \geq 6.5$ GeV/$c$, the data may be fitted by a single exponential

$$a \exp(2p\Theta/\langle p_t \rangle),$$

using a value of $\langle p_t \rangle = 0.290$ GeV/$c$. Extrapolating to zero momentum, a ratio $a = 0.05$ is obtained. The apparent break in the slope of the data is observed to occur at the minimum momentum of protons emitted in isobar decay. The dashed curve in Fig. 18 indicates the prediction on the basis of a unique distribution in transverse momentum, $\exp(2p\Theta/\langle p_t \rangle)$, using $\langle p_t \rangle = 0.44$ GeV/$c$, a value which gave a satisfactory fit to the data at angles $\Theta \geq 5^0$.[8] The striking disagreement with the experimental data invalidates the assumption of unique and independent distributions of transverse and longitudinal momentum. This is illustrated more quantitatively by comparing the mean energy loss per steradian and interaction at 0° in the c.m. system $\langle \bar{E}_0 - \bar{E}_L \rangle$, as calculated from our data,

$$\langle \bar{E}_0 - \bar{E}_L \rangle_{\text{exp}} = 2.0 \text{ GeV sr}^{-1}(\text{interaction})^{-1},$$

to the corresponding value, calculated from a spectrum at 0° as predicted, on the basis of unique and independent distributions of $p_t$ and $\bar{p}_L$, from data at larger angles, including our data at 100 mrad

$$\langle \bar{E}_0 - \bar{E}_L \rangle_{\text{pred.}} = 4.3 \text{ GeV sr}^{-1}(\text{interaction})^{-1}.$$

The striking difference may be taken as an indication that the contribution at 0° to the total mean inelasticity is reduced by a factor 2. If this result is not to affect the established value of the mean inelasticity, we have

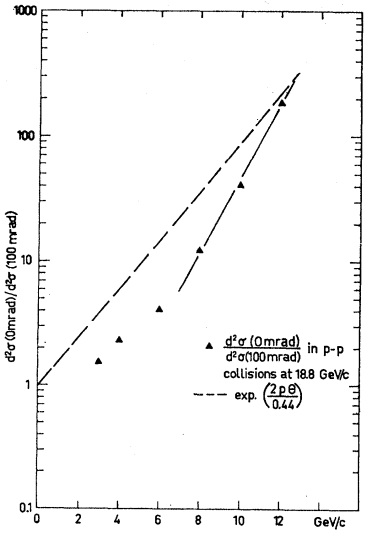


FIG. 18. Angular distribution of protons observed in $p$–$p$ collisions at 18.8 GeV/$c$. Plotted is the ratio of differential cross sections at 0 and 100 mrad versus secondary momentum. The dashed curve gives the prediction for a unique distribution in transverse momentum, using $\langle p_t \rangle = 0.44$ GeV/$c$; the solid curve is a fit to the high-momentum data with $a \exp(2p\Theta/\langle p_t \rangle)$, using $a = 0.05$ and $\langle p_t \rangle = 0.290$ GeV/$c$.

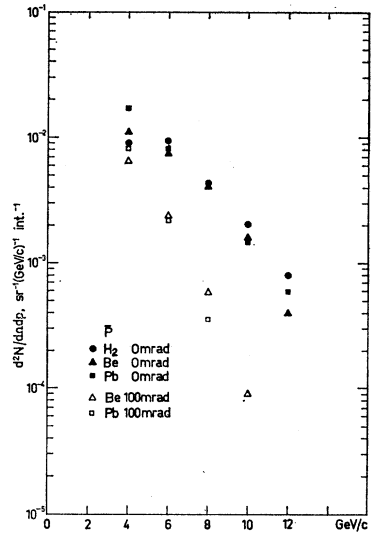


FIG. 19. Probability of antiproton production per interaction versus secondary momentum as observed in $p$–$p$, $p$–Be, and $p$–Pb collisions at 23.1 GeV/$c$. For clarity, errors are not shown, they are given in Table VIII.

to conclude that the probability for isobar excitation at small angles around 0° is indeed reduced by the limitation in change of orbital angular momentum.

## 4. Antiproton Spectra

So far the production of antiparticles in high-energy collisions has been described by statistical theories. In comparing these calculations with experiments one meets in general the difficulty that the calculations refer to an elementary process whereas the targets in experiments are complex nuclei. For some time it was thought[30] that the discrepancies between theory[4] and experiment, in particular regarding the production of antiprotons, might partly be due to reabsorption in the same nucleus where the particle was produced. Since then, reabsorption effects in complex nuclei have been calculated on the basis of a model[31] and were found to be an order of magnitude too small to account for the observed discrepancies. This result is confirmed here by a comparison of antiproton production from hydrogen and from nuclei, as shown in Fig. 19; for the comparison the experimental data are given as probabilities per interaction.[32] One notices that the probabilities per interaction obtained with different targets are indeed very close to each other.

The shape of the spectra reflects the importance of phase-space effects: strong dependence on secondary momentum and pronounced excitation with increasing primary momentum. As an example, the yield of 10 GeV/$c$ antiprotons was found to increase by a factor of 10 as the primary momentum was raised from 18.8 to 23.1 GeV/$c$. One should notice the similarity to $K^-$ production; the ratio $\bar{p}/K^-$ is constant, equal to about 0.12, and independent of the emission angle and the primary and secondary momentum in the range covered in this experiment.

The ratio of antiprotons to negative pions, as shown in Fig. 20, decreases from $10^{-2}$ at 4 GeV/$c$, to $10^{-3}$ at 12 GeV/$c$, and increases as either the primary momentum or the angle is increased. At 4 GeV/$c$ the statistical model[4] predicts a ratio of 0.2. This prediction is valid for central collisions, in which all the c.m. energy is available for production of particles. From the preceding discussion of pion production we inferred that the colliding nucleons rather separate off before an equilibrium state containing all available energy is reached and fly away in an excited state, the remaining kinetic energy available for paricle production being in the statistical average a function of the impact parameter. The fraction of central collisions may in fact be very small, of the order of[33]

$$(\sigma_{\text{central}}(p\text{–}p)/\sigma_{\text{inel.}}(p\text{–}p)) = (\pi(\hbar/M_{p.c})^2/32 \text{ mb}) \cong 1/30.$$

Antiprotons are only produced when the remaining kinetic energy left by the colliding nucleons is high. Pions are produced in the decay of excited nucleons as well. Using the estimated fraction of central collisions, the prediction of the statistical model may be reconciled with the experimental data.

One is surprised to observe that particles such as antiprotons which are produced only in central collisions, show the same characteristic Boltzmann distribu-

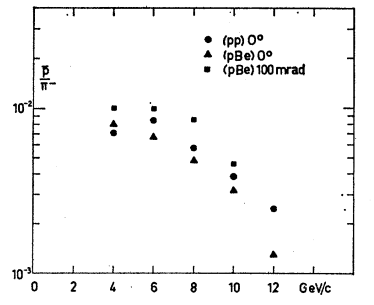


FIG. 20. Ratio of $\bar{p}/\pi^-$ versus secondary momentum as observed at 0° in $p$–$p$ collisions at 23.1 GeV/$c$ and at 0 and 100 mrad in $p$–Be collisions at 23.1 GeV/$c$.

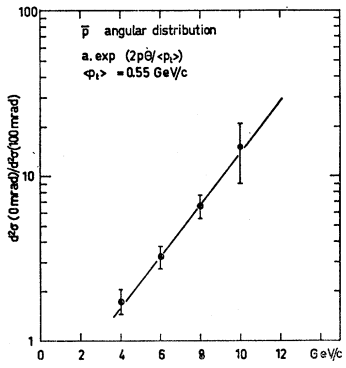


FIG. 21. Angular distribution of antiprotons produced in $p$–Be collisions at 18.8 GeV/$c$. Plotted is the ratio of differential cross sections at 0 and 100 mrad versus secondary momentum. The solid line is a fit to the data with $a \exp(2p\Theta/\langle p_t \rangle)$, using $\langle p_t \rangle = 0.55$ GeV/$c$.

[30] G. Cocconi, *Proceedings of the 1960 Annual International Conference on High-Energy Physics at Rochester* edited by E. C. G. Sudarshan, J. H. Tincot, and A. C. Melissinos (Interscience Publishers, Inc., New York, 1960), p. 801.

[31] J. Von Behr and R. Hagedorn, Nuovo Cimento **23**, 339 (1962).

[32] The following values for the inelastic cross sections were used: $\sigma_{\text{in}}(p\text{–}p) = 31$ mb, $\sigma_{\text{in}}(p\text{–Be}) = 180$ mb, $\sigma_{\text{in}}(p\text{–Pb}) = 1692$ mb.

[33] G. Cocconi, Nuovo Cimento **33**, 643 (1964).

tion of transverse momentum as particles emitted in the decay of excited nucleons. The ratio of antiproton fluxes measured at 0 and 100 mrad, as plotted against secondary momentum in Fig. 21, is indeed well fitted by an exponential corresponding to an average transverse momentum $\langle p_t \rangle = 0.55$ GeV/$c$.

Central collisions seem to be distinguished from peripheral collisions only by the occurrence of higher transverse momenta.[34]

## IV. CONCLUSIONS

Several experimental studies[12] provided information about the dynamics of isobars excitation in high energy near elastic proton scattering. Here we investigated the role of isobars in the production of secondary particles. It was found that at small angles around $0^0$ the production of positive pions is predominantly due to the decay of isobars. Negative pions were not found to be emitted in the decay by emission of a single pion. This result was shown to imply that the incident nucleon conserves the same charge in the excited state. It is equivalent to say that the exchange process responsible for isobar excitation at high energy does not change the isospin. This result seems to be of general validity in high-energy interactions.[13] Independently, the same result was derived from the observation that the number of protons per steradian at $0^0$ does not depend on the charge of the target nucleon. We can also rule out strong occurrence of simultaneous excitation of the incident and of the target nucleon to states of isospin $\frac{3}{2}$; this possibility could not be excluded in previous experiments.[12]

The high probability for isobar excitation leads us then to conclude that the colliding nucleons rather separate off before an equilibrium state containing all available energy is reached and go on in an excited state. The kinetic energy remaining in the collision rest system is in the statistical average a function of the impact parameter. Experimentally we found that the production of pions in the collision rest system increased with increasing angle.

Also positive kaons at small angles were observed to emerge predominantly from isobars decaying into $K^+\Lambda_0$. The known branching ratio[22,28] for isobar decay into positive pion and kaon gives quantitative agreement with the observed ratio $K^+/\pi^+$ at small angles; this ratio is predicted to be constant at all primary energies where the parent isobar is strongly excited. Direct excitation of strange isobars[14] can be ruled out on the basis of the observed spectrum of negative kaons.

Previous experiments[25] on the angular distribution of secondaries produced in nucleon-nucleon collisions have demonstrated as a common feature a unique distribution of transverse momentum around an average value, according to a Boltzmann law. The average transverse momentum was found to be independent of the longitudinal momentum at larger angles.[8] Here we could show that in particle production at small angles, which is dominated by isobar decay, this appears to be the result of a strange accident, produced by the combined action of dynamics, in the production of isobars, and of kinematics, in their decay. In fact an exception to the rule was found for protons. However, this exception was demonstrated to be produced by the particular dynamics of isobar excitation at $0^0$; the probability to excite the incident nucleon at $0^0$ was found to be reduced. We have tentatively interpreted this phenomenon by a limitation in the orbital angular-momentum change imposed at $0^0$. Isobars are known to have high spin values. Their excitation therefore requires a change in orbital angular momentum. At $0^0$ the probability to change the orbital angular momentum by one or more units is reduced.

An indication that the excitation of colliding nucleons remains important and of roughly constant probability up to cosmic ray energies may be found in the experimental fact that high-energy collisions are characterized by small mean inelasticities. To account for this observation one has to invoke a process in which the nucleon retains a large fraction of its primary energy. Guided by the experimental evidence at accelerator energies presented here and on the basis of cosmic-ray data[14] at 3000 GeV, we tentatively identify this process at all energies with the excitation of colliding nucleons. The observed small inelasticity then limits the mass of strongly contributing isobars to less than $2M_p$.[14] This is certainly a very strange observation. It would be much more natural to assume that there is a continuous transition from isobars of increasing mass to central collisions. If the spin of isobars continued to increase with the mass, the reduced probability for changing the orbital angular momentum by the amount required to excite a high-mass isobar at small angles could be effective to limit the mass of strongly contributing isobars. The limitation of isobar mass inferred from the small inelasticity is of course the basis of the model for particle production which was discussed here.

## ACKNOWLEDGMENTS

This investigation was originally started to provide information on pion and kaon production for an improved calculation of the neutrino spectrum in the CERN neutrino experiment. We wish to thank Professor Van Hove, Professor Preiswerk, and Professor Puppi for their interest in extending the aim of this study to a more general investigation of particle production at small angles.

The CERN proton synchrotron division has contributed a great effort to this experiment; we wish to acknowledge gratefully their whole-hearted collaboration. We also thank L. Velati and B. Friend for their assistance in setting up and running the experiment, and R. Tannenbaum for his help during the data taking.

[34] This point will be discussed in connection with experimental data on deuteron production in proton-proton collisions in a later publication.

## APPENDIX

Measured cross sections for production of $\pi^{\pm}$, $K^{\pm}$, $p$, $\bar{p}$ at 0 to 100 mrad from $p$–$p$, $p$–Be and $p$–Pb interactions at 18.8 and 23.1 GeV/$c$ are given in Tables III–VIII.

TABLE III. Positive pion production. $d^2\sigma/d\Omega dp$, mb sr$^{-1}$ (GeV/$c$)$^{-1}$ per nucleus.

| Production parameters | | | Momentum[a] of secondaries (GeV/$c$) | | | | | | | |
|---|---|---|---|---|---|---|---|---|---|---|
| Target | Angle (mrad) | Primary momentum (GeV/$c$) | 1 | 2 | 3 | 4 | 6 | 8 | 10 | 12 |
| $H_2$ | 0 | 18.8 | 28.2±3.5 | 35.5±3.5 | 52.0±5.0 | 60.0±5.0 | 83.0±6.0 | 56.0±7.0 | 24.5±1.7 | 11.9±0.8 |
| $H_2$ | 0 | 23.1 | | | | 60.0±4.5 | 86.2±6.5 | 80.4±5.5 | 46.4±3.0 | 30.6±2.0 |
| $H_2$ | 100 | 18.8 | | 38.8±4.0 | 26.2±2.4 | 19.6±1.4 | 7.71±0.49 | 2.02±0.13 | 0.54±0.03 | 0.083±0.005 |
| Be | 0 | 18.8 | 240±29 | 300±30 | 370±37 | 376±35 | 448±35 | 305±40 | 138±10 | 61±4 |
| Be | 0 | 23.1 | | | | 341±28 | 428±32 | 380±28 | 233±16 | 154±11 |
| Be | 100 | 18.8 | | 297±35 | 207±18 | 135±10 | 49±3 | 13.0±0.8 | 3.1±0.2 | 0.42±0.03 |
| Be | 100 | 23.1 | | | | 168±12 | 70±5 | 24.5±1.6 | 7.1±0.45 | 1.39±0.09 |
| Pb | 0 | 18.8 | 4070±500 | 3900±400 | 4200±420 | 3380±260 | 3460±230 | 2100±135 | 990±65 | 390±26 |
| Pb | 0 | 23.1 | | | | 3660±280 | 3860±270 | 2940±195 | 1790±120 | 1170±80 |
| Pb | 100 | 23.1 | | | | 1810±130 | 712±46 | 247±16 | 79±5 | 15.9±1 |

[a] Errors quoted are due to systematic uncertainties.

TABLE IV. Negative pion production. $d^2\sigma/d\Omega dp$, mb sr$^{-1}$ (GeV/$c$)$^{-1}$ per nucleus.

| Production parameters | | | Momentum[a] of secondaries (GeV/$c$) | | | | | | | |
|---|---|---|---|---|---|---|---|---|---|---|
| Target | Angle (mrad) | Primary momentum (GeV/$c$) | 1 | 2 | 3 | 4 | 6 | 8 | 10 | 12 |
| $H_2$ | 0 | 18.8 | 26.2±3.2 | 30.0±3.0 | 34.0±3.4 | 28.0±4.0 | 21.6±1.7 | 13.3±0.9 | 7.8±0.5 | 2.45±0.15 |
| $H_2$ | 0 | 23.1 | | | | 39.0±4.0 | 34.1±2.5 | 23.6±1.5 | 16.2±1.2 | 9.9±0.7 |
| $H_2$ | 100 | 18.8 | | 22.5±2.5 | 17.9±1.6 | 10.6±1.0 | 3.75±0.27 | 1.06±0.07 | 0.21±0.014 | 0.023±0.0014 |
| Be | 0 | 18.8 | 229±26 | 273±27 | 265±27 | 215±30 | 152±13 | 92±7 | 50.0±3.5 | 15.4±1.2 |
| Be | 0 | 23.1 | | | | 267±27 | 211±16 | 157±12 | 94.4±6.5 | 54.9±4.5 |
| Be | 100 | 18.8 | | 296±32 | 144±13 | 82.8±7.7 | 29.1±2.1 | 7.76±0.53 | 1.56±0.1 | 0.187±0.012 |
| Be | 100 | 23.1 | | | | 125±11 | 46.1±3.3 | 14.2±1.0 | 3.73±0.25 | 0.72±0.05 |
| Pb | 0 | 18.8 | 4000±500 | 3420±340 | 2970±300 | 2080±290 | 1290±100 | 680±50 | 340±24 | 107 ±7 |
| Pb | 0 | 23.1 | | | | 2790±260 | 1940±150 | 1200±85 | 714±52 | 400±30 |
| Pb | 100 | 23.1 | | | | 1360±125 | 470±34 | 146±10 | 38.0±2.5 | 7.7±0.5 |

[a] Errors quoted are due to systematic uncertainties.

TABLE V. Positive kaon production. $d^2\sigma/d\Omega dp$, mb sr$^{-1}$ (Ge=/$c$)$^{-1}$ per nucleus.

| Production parameters | | | Momentum[a] of secondaries (GeV/$c$) | | | | |
|---|---|---|---|---|---|---|---|
| Target | Angle (mrad) | Primary momentum (GeV/$c$) | 4 | 6 | 8 | 10 | 12 |
| $H_2$ | 0 | 18.8 | 3.18± 0.60 | 4.26± 0.70 | 3.09± 0.40 | 2.62 ± 0.70 | 0.98 ± 0.11 |
| $H_2$ | 0 | 23.1 | 5.00± 0.85 | 5.55± 0.72 | 4.27± 0.48 | 4.00 ± 0.56 | 2.21 ± 0.63 |
| $H_2$ | 100 | 18.8 | 1.7 ± 0.2 | 0.80± 0.11 | 0.21± 0.02 | 0.056± 0.007 | 0.008± 0.004 |
| Be | 0 | 18.8 | 30.2 ± 3.4 | 29.5 ± 4.8 | 18.5 ± 3.0 | 14.8 ± 6.0 | 7.6 ± 1.2 |
| Be | 0 | 23.1 | 32.9 ± 3.0 | 38.9 ± 5.3 | 25.8 ± 2.8 | 24.1 ± 3.2 | 11.3 ± 3.8 |
| Be | 100 | 18.8 | 16.3 ± 1.4 | 6.8 ± 0.5 | 1.9 ± 0.14 | 0.55 ± 0.05 | 0.046± 0.01 |
| Be | 100 | 23.1 | 21.0 ± 1.8 | 10.6 ± 0.7 | 3.9 ± 0.3 | 1.04 ± 0.09 | 0.21 ± 0.03 |
| Pb | 0 | 18.8 | 421 ±67 | 281 ±76 | 235 ±63 | | 62 ±13 |
| Pb | 0 | 23.1 | 469 ±75 | 520 ±88 | 260 ±52 | 234 ±54 | |
| Pb | 100 | 23.1 | 295 ±24 | 148 ±13 | 57.0 ± 5.0 | 18.0 ± 1.6 | 3.50 ± 0.37 |

[a] Errors quoted include both statistical and systematic uncertainties.

TABLE VI. Negative kaon production. $d^2\sigma/d\Omega dp$, mb sr$^{-1}$ (GeV/$c$)$^{-1}$ per nucleus.

| Production parameters | | | | | | | |
|---|---|---|---|---|---|---|---|
| | | | Momentum[a] of secondaries (GeV/$c$) | | | | |
| Target | Angle (mrad) | Primary momentum (GeV/$c$) | 4 | 6 | 8 | 10 | 12 |
| $H_2$ | 0 | 18.8 | 1.18± 0.46 | 0.83± 0.16 | 0.34 ±0.03 | 0.09 ±0.02 | 0.055±0.010 |
| $H_2$ | 0 | 23.1 | 3.03± 0.61 | 1.92± 0.29 | 0.93 ±0.09 | 0.56 ±0.05 | 0.20 ±0.02 |
| $H_2$ | 100 | 18.8 | 1.16± 0.14 | 0.31± 0.03 | 0.037±0.005 | | |
| Be | 0 | 18.8 | 13.1 ± 1.4 | 6.75± 0.71 | 3.13 ±0.25 | 0.902±0.062 | 0.168±0.027 |
| Be | 0 | 23.1 | 20.5 ± 2.7 | 11.8 ± 1.1 | 5.98 ±0.47 | 3.37 ±0.24 | 1.16 ±0.09 |
| Be | 100 | 18.8 | 7.3 ± 0.8 | 2.30± 0.20 | 0.25 ±0.02 | 0.031±0.005 | |
| Be | 100 | 23.1 | 13.3 ± 1.2 | 3.90± 0.30 | 0.63 ±0.06 | 0.14 ±0.015 | 0.017±0.004 |
| Pb | 0 | 18.8 | 169 ±35 | 73 ±12 | 30.0 ±4.4 | 6.46 ±1.30 | 2.50 ±0.65 |
| Pb | 0 | 23.1 | 304 ±52 | 177 ±20 | 68.0 ±5.0 | 27.7 ±2.8 | 7.62 ±1.10 |
| Pb | 100 | 23.1 | 153 ±16 | 44.0 ± 4.4 | 7.80 ±0.90 | 1.36 ±0.21 | 0.31 ±0.10 |

[a] Errors quoted include both statistical and systematic uncertainties.

TABLE VII. Proton spectra. $d^2\sigma/d\Omega dp$, mb sr$^{-1}$ (GeV/$c$)$^{-1}$ per nucleus.

| Production parameters | | | | | | | | | | |
|---|---|---|---|---|---|---|---|---|---|---|
| | | | Momentum[a] of secondaries (GeV/$c$) | | | | | | | |
| Target | Angle (mrad) | Primary momentum (GeV/$c$) | 1 | 2 | 3 | 4 | 6 | 8 | 10 | 12 |
| $H_2$ | 0 | 18.8 | 5.0±0.6 | | 14.0±1.3 | 24.2±2.0 | 48.4±3.4 | 95.1±6.6 | 170±12 | 267±18 |
| $H_2$ | 0 | 23.1 | | | | 25.8±2.2 | 39.4±2.9 | 70.0±4.9 | 102±7 | 151±10 |
| $H_2$ | 100 | 18.8 | | | 9.1±0.8 | 10.6±0.9 | 11.4±0.8 | 7.73±0.53 | 4.19±0.28 | 1.44±0.1 |
| Be | 0 | 18.8 | 57.0±6.5 | | 136±11 | 208±19 | 362 ±26 | 614±43 | 903±61 | 1340±91 |
| Be | 0 | 23.1 | | | | 164±14 | 251±18 | 444±31 | 652±44 | 959±80 |
| Be | 100 | 18.8 | | | 94.5±8.5 | 103±9 | 99.4±7.3 | 59.7±4.2 | 30.3±2.1 | 10.1±0.6 |
| Be | 100 | 23.1 | | | | 94.4±7.9 | 90.6±6.6 | 61.0±4.3 | 31.8±2.2 | 12.9±0.9 |
| Pb | 0 | 18.8 | 1910±230 | | 2117±200 | 2870±240 | 3550±250 | 5100±350 | 6440±430 | 8700±580 |
| Pb | 0 | 23.1 | | | | 2510±210 | 2870±210 | 4090±280 | 5210±350 | 7150±480 |
| Pb | 100 | 23.1 | | | | 1460±120 | 1100±80 | 720±50 | 400±27 | 160 11 |

[a] Errors quoted are due to systematic uncertainties.

TABLE VIII. Antiproton production. $d^2\sigma/d\Omega dp$, mb sr$^{-1}$ (GeV/$c$)$^{-1}$ per nucleus.

| Production parameters | | | | | | | |
|---|---|---|---|---|---|---|---|
| | | | Momentum[a] of secondaries (GeV/$c$) | | | | |
| Target | Angle (mrad) | Primary momentum (GeV/$c$) | 4 | 6 | 8 | 10 | 12 |
| $H_2$ | 0 | 18.8 | 0.154±0.046 | 0.077±0.022 | | | |
| $H_2$ | 0 | 23.1 | 0.281±0.055 | 0.291±0.042 | 0.137 ±0.018 | 0.063 ±0.012 | 0.025±0.006 |
| $H_2$ | 100 | 18.8 | 0.063±0.020 | 0.032±0.008 | 0.0054±0.0015 | | |
| Be | 0 | 18.8 | 1.04 ±0.17 | 0.62 ±0.10 | 0.19 ±0.04 | 0.048 ±0.019 | |
| Be | 0 | 23.1 | 2.08 ±0.33 | 1.41 ±0.19 | 0.76 ±0.08 | 0.306 ±0.035 | 0.073±0.015 |
| Be | 100 | 18.8 | 0.531±0.100 | 0.191±0.017 | 0.029 ±0.004 | 0.0032±0.001 | |
| Be | 100 | 23.1 | 1.22 ±0.20 | 0.460±0.064 | 0.122 ±0.017 | 0.017 ±0.005 | |
| Pb | 0 | 18.8 | 12.2 ±3.3 | 4.80 ±1.40 | 2.00 ±0.60 | | |
| Pb | 0 | 23.1 | 28.7 ±4.9 | 14.1 ±2.7 | 7.20 ±1.00 | 2.40 ±0.75 | 1.00 ±0.50 |
| Pb | 100 | 23.1 | 14.0 ±2.3 | 3.80 ±0.70 | 0.61 ±0.24 | | |

[a] Errors quoted include both statistical and systematic uncertainties.

TABLE IX. Positive pion production. $d^2\sigma/d\Omega dp$, mb sr$^{-1}$ (GeV/$c$)$^{-1}$ per nucleus.

| Production parameters | | | | | | |
|---|---|---|---|---|---|---|
| | | | Momentum of secondaries (GeV/$c$) | | | |
| Target | Angle (mrad) | Primary momentum (GeV/$c$) | 4 | 5 | 6 | 7 |
| Be | 0 | 8.65 | 58±12 | | | |
| Be | 0 | 11.8 | 318±64 | 142±28 | 90±18 | 42±8 |

TABLE X. Negative pion production. $d^2\sigma/d\Omega dp$, mb sr$^{-1}$ (GeV/$c$)$^{-1}$ per nucleus.

| Target | Production parameters: Angle (mrad) | Primary momentum (GeV/$c$) | Momentum of secondaries (GeV/$c$): 4 | 5 | 6 | 7 |
|---|---|---|---|---|---|---|
| Be | 0 | 8.65 | 35±7 | | | |
| Be | 0 | 11.8 | 124±25 | 91±18 | 43±9 | 20±4 |

TABLE XI. Proton spectra. $d^2\sigma/d\Omega dp$, mb sr$^{-1}$ (Ge=/$c$)$^{-1}$ per nucleus.

| Target | Production parameters: Angle (mrad) | Primary momentum (GeV/$c$) | Momentum of secondaries (GeV/$c$): 4 | 5 | 6 | 7 |
|---|---|---|---|---|---|---|
| Be | 0 | 8.65 | 244±65 | | | |
| Be | 0 | 11.8 | 263±50 | 390±70 | 575±110 | 885±180 |

PHYSICAL REVIEW VOLUME 137, NUMBER 4B 22 FEBRUARY 1965

# Electron Helicity in the Final State of Elastic *e-p* and *e-d* Scattering

G. RAMACHANDRAN* AND R. K. UMERJEE†
*The Institute of Mathematical Sciences, Madras, India*

(Received 3 September 1964; revised manuscript received 22 October 1964)

The percentage helicity of high-energy electrons scattered by target polarized protons and deuterons is discussed assuming one-photon exchange. With target protons polarized parallel to the direction of the incident beam, the back-scattered electrons get 100% polarized, which is expected to be of considerable experimental interest as a method of producing polarized electrons. Taking into account all possible types of deuteron target polarization, it is found that the percentage helicity of the final electrons is nonzero only if the targets are linearly polarized, and the relevance of this process to the study of the electromagnetic form factors of the neutron is also discussed.

## 1. INTRODUCTION

THE study of scattering of high-energy electrons by nucleons constitutes our main source of knowledge of the nucleon electromagnetic form factors. Elastic as well as inelastic scattering of electrons from deuterons have been discussed extensively in the context of determining the neutron form factors The polarization of the nucleon in the inelastic scattering by deuteron has been considered by Durand,[1] while more recently the deuteron polarization in the elastic case as also the possibilities of using polarized deuterons as targets have been considered theoretically by Schildknecht and Gourdin *et al.*, respectively.[2,3] While it is yet too early to visualize experiments using polarized deuterons, attempts have already been made[4] with some success to obtain target polarized protons.

An interesting feature of the scattering of electrons by polarized targets is the helicity of the electron in the final state. We discuss in this paper the electron helicity in the final state of $e+p \rightarrow e+p$ and $e+d \rightarrow e+d$ taking into account all possible forms of target polarization. We assume the processes to proceed through one-photon exchange and the method of calculation here makes use of the nonrelativistic trace method[5,6] to treat the spin-$\frac{1}{2}$

* Council of Scientific and Industrial Research, India, Senior Research Fellow.

† Council of Scientific and Industrial Research, India, Junior Research Fellow.

[1] Loyal Durand III, Phys. Rev. **123**, 1392 (1961).

[2] D. Schildknecht, Phys. Letters **10**, 254 (1964).

[3] M. Gourdin and C. A. Piketty, Nuovo Cimento **32**, 1137 (1964).

[4] E. Segrè, Lectures given at the Institute of Mathematical Sciences, Madras, 1962 MATSCIENCE Report 18 (unpublished). L. J. B. Goldfarb and D. A. Bromley, *Proceedings of the Conference on Direct Interactions and Nuclear Reaction Mechanisms, Padua, 1962* (Gordon and Breach Science Publishers, Inc., New York, 1964), p. 609; A. Abragam, M. Borghini, P. Catillion, J. Coustham, P. Roubeau, and J. Thirion, *ibid.* p. 617.

[5] L. Wolfenstein, Ann. Rev. Nucl. Sci. **6**, 43 (1953). G. Ramachandran, Lectures on Angular momentum, MATSCIENCE Report 2, 1962 (unpublished), p. 105.

[6] G. Ramachandran and R. K. Umerjee, Nucl. Phys. **54**, 665 (1964); The last two lines of Eq. (20) in this paper should read as

$$\langle T_{\pm 1}{}^2\rangle = \mp 2^{-1/2}[\langle s^5\rangle \pm i\langle s^6\rangle]; \quad \langle T_{\pm 2}{}^2\rangle = 2^{-1/2}[\langle s^8\rangle \pm i\langle s^4\rangle].$$

R. K. Umerjee, Nucl. Phys. (to be published).